NASA TM X-436

TECHNICAL MEMORANDUM

X-436

LOW-SPEED INVESTIGATION OF EFFECTS OF VERTICAL TAILS ON THE STATIC STABILITY CHARACTERISTICS OF A CANARD-BOMBER CONFIGURATION HAVING A VERY THIN WING AND A SLENDER ELLIPTICAL FUSELAGE

By Thomas G. Gainer

Langley Research Center
Langley Field, Va.

[redacted]

NATIONAL AERONAUTICS AND SPACE ADMINISTRATION

WASHINGTON

January 1961

lW

NATIONAL AERONAUTICS AND SPACE ADMINISTRATION

TECHNICAL MEMORANDUM X-436

LOW-SPEED INVESTIGATION OF EFFECTS OF VERTICAL TAILS ON THE STATIC STABILITY CHARACTERISTICS OF A CANARD-BOMBER CONFIGURATION HAVING A VERY THIN WING AND A SLENDER ELLIPTICAL FUSELAGE*

By Thomas G. Gainer

SUMMARY

An investigation has been made of the low-speed static stability characteristics of a canard-bomber configuration having a very thin wing and a slender fuselage of elliptical cross section. The wing of the model had an aspect ratio of 1.67, a taper ratio of 0.25, a sweep of the 1/4-chord line of 56.8°, and a 2-percent-thick hexagonal airfoil section. Tests were made through an angle-of-attack range of approximately -2° to 20° and over a sideslip-angle range of -4° to 10°. The model was tested with and without small and large vertical tails attached at the wing tips. Some tests were also made with the canard surfaces removed.

The results of the investigation indicated that the model was longitudinally stable without vertical tails throughout the test angle-of-attack range; and adding either the small or large vertical tails produced some reductions in stability at the higher lift coefficients. There was little variation in the longitudinal characteristics of the model with varying sideslip angle at 9° angle of attack. With vertical tails off the model had a very small amount of directional instability at low angles of attack but became slightly stable as the angle of attack was increased above about 8°. Adding either the small or large vertical tails provided directional stability at all test angles of attack. The model had positive effective dihedral at positive angles of attack for all configurations tested. Removing the canard surface at 9° angle of attack tended to reduce the negative values of side-force parameter C_{Y_β} and to increase the positive values of directional-stability parameter C_{n_β} obtained with canard surface on.

*Title, Unclassified.

INTRODUCTION

Much of the current effort in the field of aircraft design is being directed toward developing aircraft with long-range cruise capabilities at a Mach number of 3. One of the configurations proposed for this purpose was investigated in the Langley Unitary Plan wind tunnel at supersonic speeds; the study indicated that lift-drag ratios of the order of 7.0 could be obtained at Reynolds numbers of 3 or 4 million at Mach numbers near 3. These results were obtained for a canard configuration having a very thin wing and a slender fuselage of elliptical cross section. The concept followed in designing this model was to achieve high lift-drag ratios by minimizing the zero-lift drag, with the frontal area being minimized within the requirements for a possible supersonic bomber configuration. This paper presents some low-speed static stability characteristics of this canard-bomber configuration.

The model was tested in the Langley 300-MPH 7- by 10-foot tunnel at a Reynolds number of 2.38×10^6, based on the model mean aerodynamic chord of 1.151 feet. Tests were made through an angle-of-attack range of approximately -2° to 20° and over a sideslip-angle range of -4° to 10°. The model was tested without vertical tails and with small and large vertical tails attached at the wing tips. Some tests were also made with the canard surfaces removed.

SYMBOLS

Forces and moments are referred to the system of axes shown in figure 1. All moments are measured about a center-of-gravity position located at 12.3 percent of the mean aerodynamic chord at a distance 1.01 percent of the mean aerodynamic chord below the wing-chord plane at the plane of symmetry.

X,Y,Z coordinate axes

C_D drag coefficient, F_D/qS

C_L lift coefficient, F_L/qS

C_l rolling-moment coefficient, M_X/qSb

$$C_{l_\beta} = \frac{\partial C_l}{\partial \beta}\left(\text{calculated as } \frac{C_{l_{\beta=4^\circ}} - C_{l_{\beta=-4^\circ}}}{8}\right), \text{ per deg}$$

C_m pitching-moment coefficient, $M_Y/qS\bar{c}$

C_n yawing-moment coefficient, M_Z/qSb

$C_{n_\beta} = \frac{\partial C_n}{\partial \beta}$ $\left(\text{calculated as } \frac{C_{n_{\beta=4^o}} - C_{n_{\beta=-4^o}}}{8}\right)$, per deg

C_Y lateral-force coefficient, F_Y/qS

$C_{Y_\beta} = \frac{\partial C_Y}{\partial \beta}$ $\left(\text{calculated as } \frac{C_{Y_{\beta=4^o}} - C_{Y_{\beta=-4^o}}}{8}\right)$, per deg

L 1 2 3 9

b wing span, ft

c wing chord, ft

$\bar{c}$ wing mean aerodynamic chord, ft

F_D drag force, lb

F_L lift force, lb

F_Y side force, lb

M_X rolling moment, ft-lb

M_Y pitching moment, ft-lb

M_Z yawing moment, ft-lb

q dynamic pressure, $\rho V^2/2$, lb/sq ft

S wing area, sq ft

V airspeed, ft/sec

α angle of attack, deg

β angle of sideslip, deg

ρ air density, slugs/cu ft

APPARATUS AND MODEL

The tests were made in the Langley 300-MPH 7- by 10-foot tunnel with a sting-support system and an internally mounted six-component strain-gage balance. A three-view drawing of the model is shown in figure 2(a) and details of the small and large vertical tails tested are given in figure 2(b). The model with large vertical tails is shown mounted in the tunnel in figures 3(a) and 3(b). The model wing had an aspect ratio of 1.67, a taper ratio of 0.25, and a sweep of the 1/4-chord line of 56.8°. The mean aerodynamic chord of the wing was 1.151 feet, the span was 1.727 feet, and the area was 1.783 square feet. The wing had a hexagonal airfoil section having a maximum thickness of 2 percent of the chord with ridge lines at 0.50c and 0.70c.

The canard surface of the model had a double-wedge section having a maximum thickness of 2 percent of the canard-surface chord. The area of the canard surface, including the area covered by the fuselage, amounted to 8.2 percent of the total wing area. Each small vertical tail had an area equal to 2.9 percent of the wing area and each large vertical tail had an area of 5.8 percent of the wing area. These tails were attached to the wing tips in the positions indicated in figure 2(a). The fuselage of the model was elliptical in cross section and the portion from approximately the 63-percent fuselage station forward to the 42-percent fuselage station was bent at an angle of 6° with respect to the remainder of the fuselage. The purpose of this bend is to raise the canard surface above the wing-chord plane to reduce interference between the canard-surface wake and the wing and to improve the longitudinal trim characteristics at supersonic speeds with an increment in pitching moment produced by the added camber of the fuselage. The fuselage was constructed of aluminum and the wing, canard surface, and vertical tails were constructed of stainless steel.

The model was equipped with two engine ducts each having an inlet area and exit area equal to 0.00895 square foot. The base area of the model, including the area occupied by the sting but not including the duct exit areas, was 0.0357 square foot.

TESTS

Tests were made at a dynamic pressure of 125 pounds per square foot, which corresponds to an airspeed of about 324 feet per second at standard sea-level conditions (Mach number, 0.29) and a Reynolds number of approximately 2.38×10^6 based on the model mean aerodynamic chord of 1.151 feet. Three model configurations were tested: one with the vertical tails off, one with the small vertical tails on, and one with the large vertical

tails on. Lateral stability derivatives were obtained from tests through an angle-of-attack range from approximately -2° to 20° at fixed sideslip angles of $\pm 4^\circ$. Tests were made at 0° sideslip through the angle-of-attack range to obtain the longitudinal characteristics of the three configurations. Tests were also made at angles of attack of approximately 0°, 9°, and 18° with the angle of sideslip varying from -4° to 10°. In addition, the model was tested with the canard surface removed at 9° angle of attack with varying angles of sideslip.

CORRECTIONS

Jet-boundary corrections were applied to the data as indicated by the following equations:

$$\alpha = \alpha_{tunnel} + K_1 C_L$$

$$C_D = C_{D,measured} + K_2 C_L^2$$

For tests in which the angle of attack was varied at a fixed angle of sideslip, the model was mounted with the wing vertical in the tunnel and the constants K_1 and K_2 used in the preceding equations were determined by the method of reference 1, with an elliptic distribution of lift being assumed. For tests in which the angle of sideslip was varied at a fixed angle of attack, the model was mounted with the wing horizontal in the tunnel and K_1 and K_2 were determined by the method of reference 2. Large displacements of the model lifting line above the horizontal center line of the tunnel were also accounted for in the jet-boundary corrections. The values of K_1 and K_2 for the various test conditions are listed in the following table:

Type of test	K_1	K_2
α variable; $\beta = 0^\circ$ and $\pm 4^\circ$	0.270	0.00472
$\alpha = 0^\circ$; β variable	.172	.00300
$\alpha = 9^\circ$; β variable	.180	.00314
$\alpha = 18^\circ$; β variable	.216	.00378

Blockage corrections were negligible because of the small size of the model relative to the tunnel cross-sectional area and the relatively

low speed at which the tests were made; blockage corrections, therefore, were not applied to the data. Both the angle of attack and angle of sideslip were corrected for deflection of the sting-support system and strain-gage balance under load. The drag was also corrected to the condition of free-stream static pressure acting on the base area of the model. No corrections with regard to the internal flow through the engine ducts were made to the drag.

RESULTS AND DISCUSSION

Static Longitudinal Stability Characteristics

The static longitudinal stability characteristics of the model are presented in figure 4 for the three configurations tested. The data of figure 4 indicate that the model was longitudinally stable without vertical tails throughout the test angle-of-attack range. Adding either the small or large vertical tails had no effect on the stability near zero lift but produced some reductions in stability at the higher lift coefficients. With the large vertical tails on, the model was about neutrally stable at lift coefficients near 1.0. The slope of the pitching-moment curves at $C_L = 0$ indicates an aerodynamic-center location at about 22 percent of the mean aerodynamic chord. Adding the vertical tails generally had little effect on the lift or drag characteristics of the model, although a slightly lower lift can be noticed for the tails-on configurations at the higher angles of attack.

The effects of sideslip angle on the longitudinal characteristics of the model with vertical tails off and with and without the canard surface at $\alpha \approx 9^\circ$ are shown in figure 5; little variation in the longitudinal characteristics occurs with varying sideslip angle. Removing the canard surface doubled the magnitude of the pitching-moment coefficient at a given angle of attack but had little effect on the lift or drag.

Static Lateral Stability Characteristics

The results of tests made to determine the static lateral stability characteristics of the model with and without the small and large vertical tails through a sideslip-angle range from -4° to 10° at angles of attack of 0°, 9°, and 18° are presented in figures 6(a), 6(b), and 6(c), respectively. The static lateral stability characteristics of the model are summarized in figure 7 as the variation with angle of attack of the side-force parameter C_{Y_β}, the directional-stability parameter C_{n_β}, and the effective dihedral parameter C_{l_β}. These parameters were obtained

from tests through the angle-of-attack range from approximately -2° to 20° at ±4° angle of sideslip and, as can be seen by measuring the slopes of the curves of figure 6, are generally a good representation of the lateral stability characteristics of the model at low angles of sideslip. The data of figure 7 show that, for the tails-off configuration, values of C_{Y_β} were negative but tended to approach zero at about 16° angle of attack because of changes in the flow field over the fuselage forebody. The negative increments in C_{Y_β} produced by the vertical tails tended to increase with angle of attack and for the complete-model configurations C_{Y_β} became more negative as the angle of attack was increased. In general, figure 7 shows an increase in the directional stability of the model as the angle of attack was increased. With vertical tails off the model had a very small amount of directional instability at low angles of attack but became slightly stable as the angle of attack was increased above about 8°. Adding either the small or large vertical tails provided directional stability over the entire test angle-of-attack range. The increments in C_{n_β} produced by either small or large tails tended to increase with angle of attack and for the tails-on configurations C_{n_β} was three or four times higher at $\alpha = 20°$ than at $\alpha = 0°$. Figure 7 also shows that the model had positive effective dihedral $\left(-C_{l_\beta}\right)$ for all positive angles of attack, with the increments in C_{l_β}, produced by either set of vertical tails, being relatively small except at the higher angles of attack.

The lateral characteristics of the model with the canard surface off at 9° angle of attack are given in figure 8. By comparing the data of figures 8 and 6(b) it can be seen that removing the canard surface had little effect on C_{l_β} but tended to make both C_{Y_β} and C_{n_β} more positive. Figure 8 indicates positive values of C_{Y_β} for the vertical-tails-off configuration with the canard removed.

CONCLUSIONS

A wind-tunnel investigation to determine the low-speed static longitudinal and lateral stability characteristics of a canard-bomber configuration, with and without small and large vertical tails attached at the wing tips, indicated the following conclusions:

1. The model was longitudinally stable without vertical tails throughout the test angle-of-attack range; adding either the small or large vertical tails produced some reductions in stability at the

higher lift coefficients. There was little variation in the longitudinal characteristics of the model with varying sideslip angle at 9° angle of attack.

2. With vertical tails off the model had a very small amount of directional instability at low angles of attack but became slightly stable as the angle of attack was increased above about 8°. Adding either the small or large vertical tails provided directional stability at all test angles of attack.

3. The model had positive effective dihedral at positive angles of attack for all configurations tested.

4. Removing the canard at 9° angle of attack tended to reduce the negative values of side-force parameter C_{Y_β} and increase the positive values of directional-stability parameter C_{n_β} obtained with the canard surface on.

Langley Research Center,
National Aeronautics and Space Administration,
Langley Field, Va., October 4, 1960.

REFERENCES

1. Sanders, J., and Pounder, J. R.: Wall Interference in Wind Tunnels of Closed Rectangular Section. Aero. Rep. AR-7, Nat. Res. Council of Canada (Ottawa), 1949.

2. Gillis, Clarence L., Polhamus, Edward C., and Gray, Joseph L., Jr.: Charts for Determining Jet-Boundary Corrections for Complete Models in 7- by 10-Foot Closed Rectangular Wind Tunnels. NACA WR L-123, 1945. (Formerly NACA ARR L5G31.)

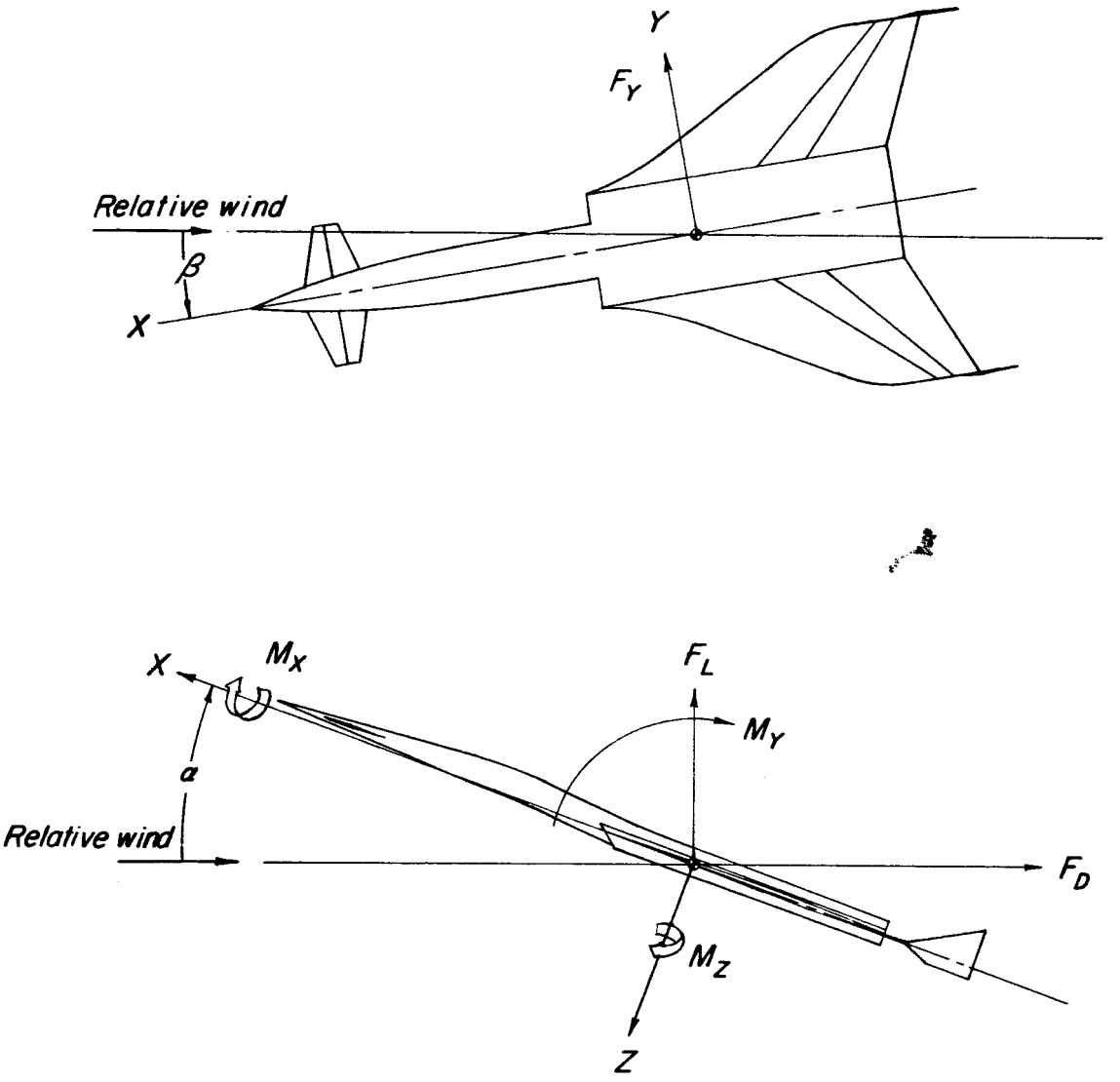

Figure 1.- Axes system and convention used to define positive sense of forces, moments, and angles.

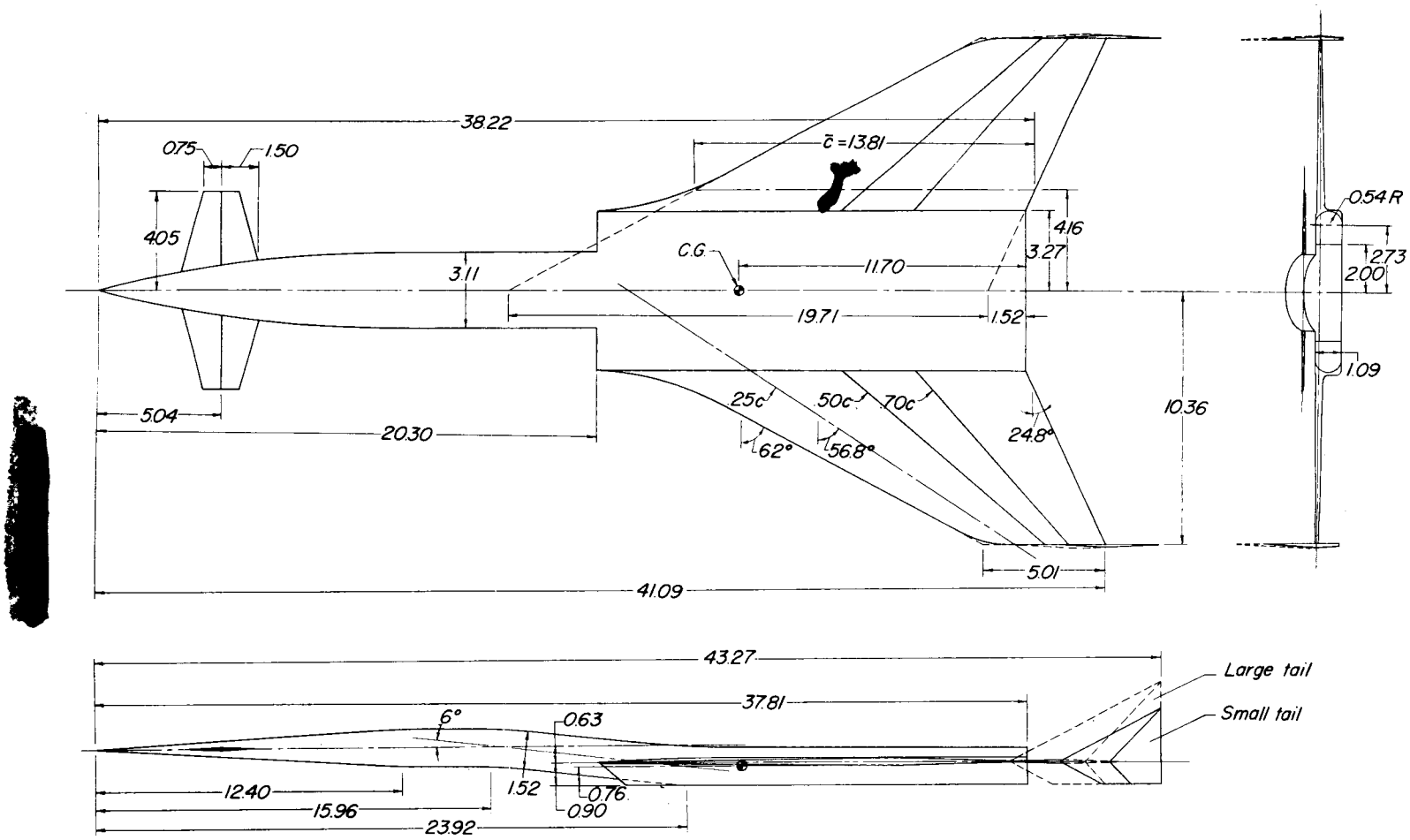

(a) Three-view drawing of model.

Figure 2.- Geometric characteristics of model. All dimensions are in inches.

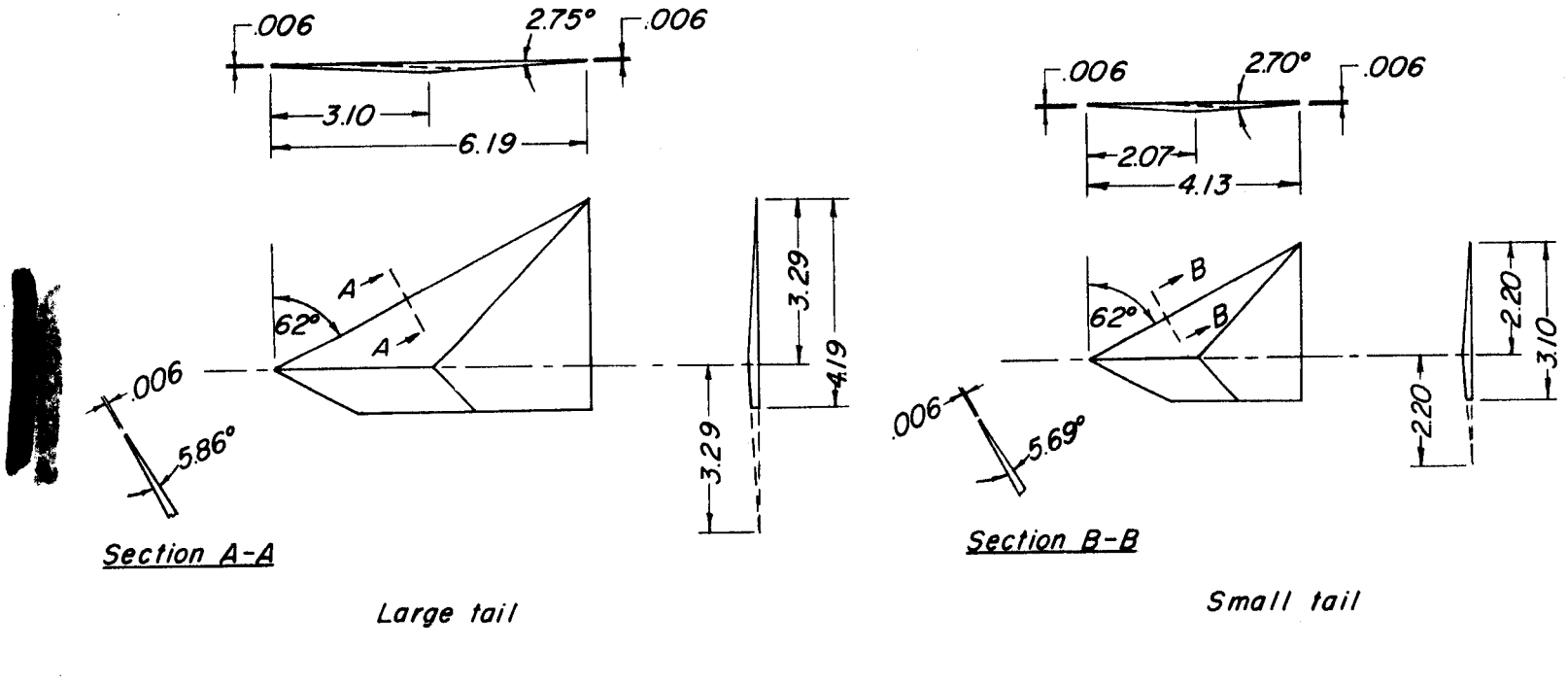

(b) Details of vertical tails tested.

Figure 2.- Concluded.

L-60-2786

(a) Three-quarter bottom view.

Figure 3.- Model installed in Langley 300-MPH 7- by 10-foot tunnel.

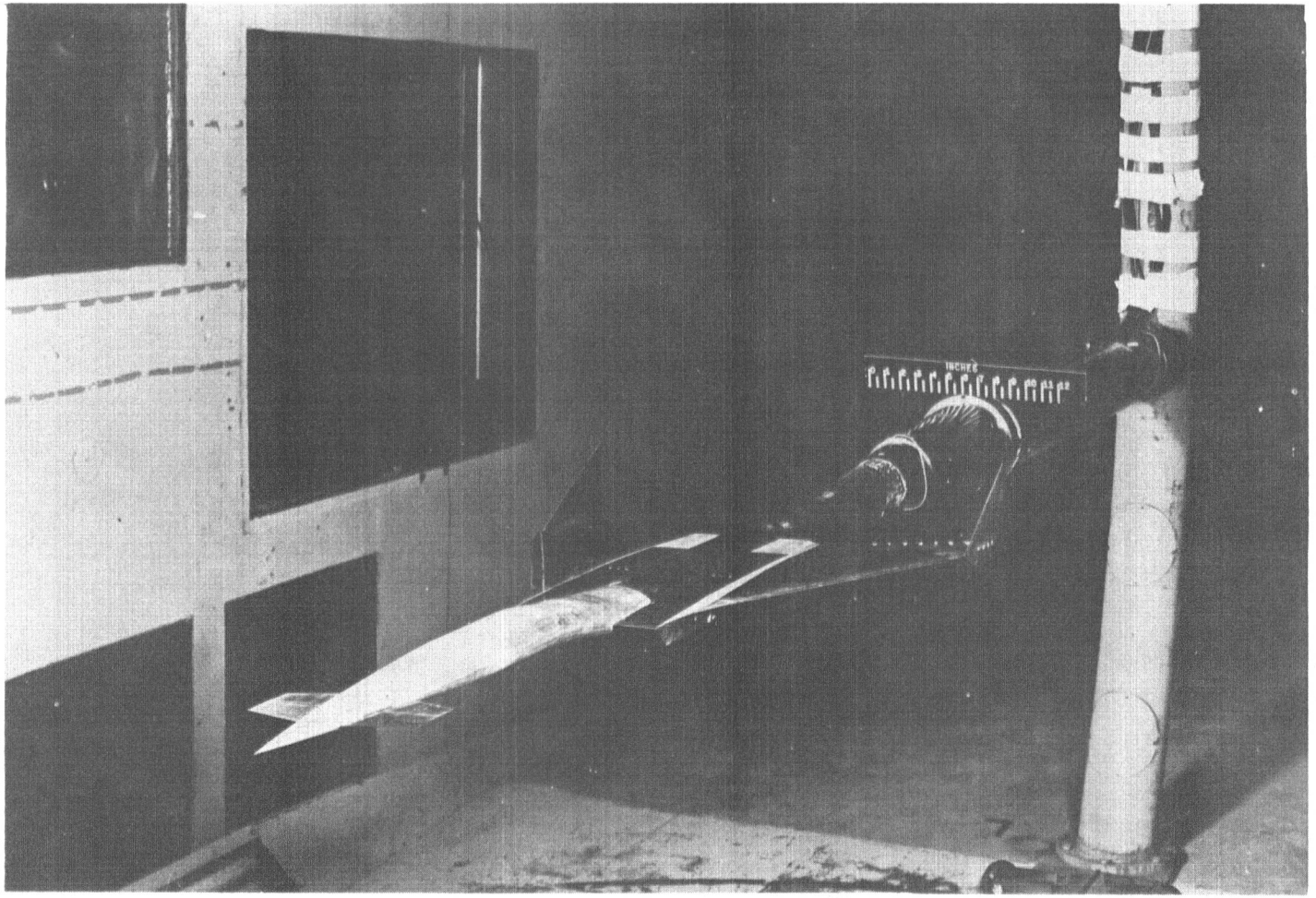

(b) Three-quarter top view. L-60-2785

Figure 3.- Concluded.

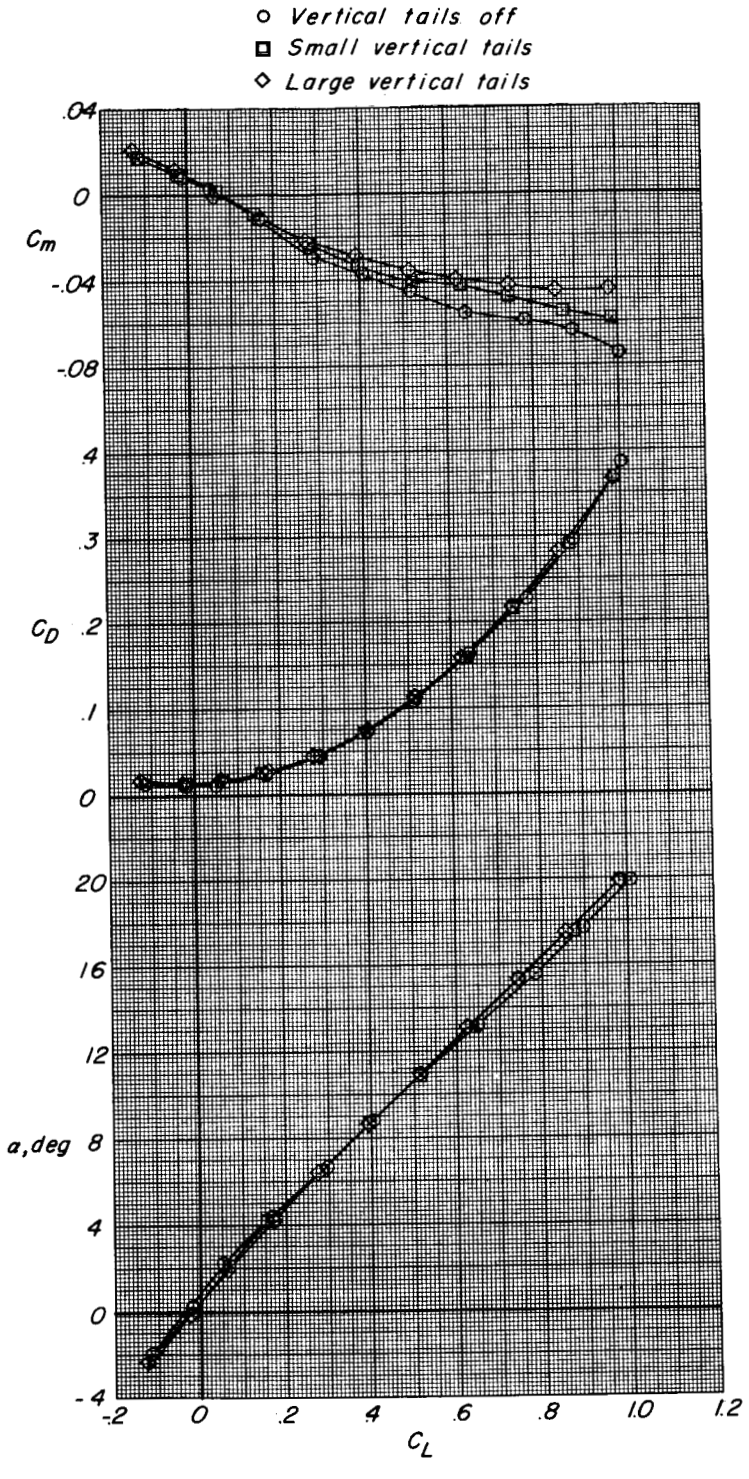

Figure 4.- Longitudinal characteristics of model.

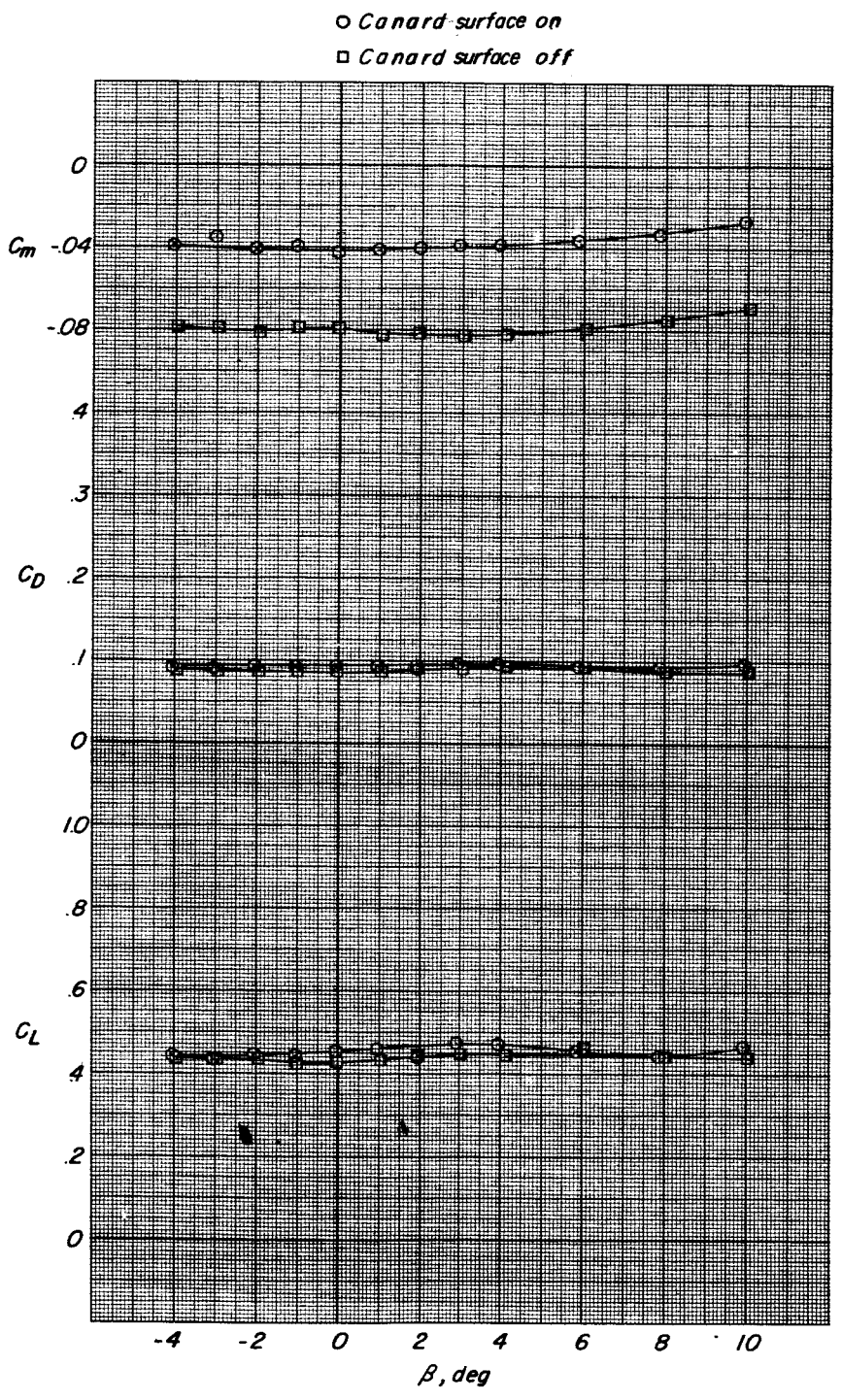

Figure 5.- Variation of static longitudinal characteristics with angle of sideslip. Vertical tails off; $\alpha \approx 9^{\circ}$.

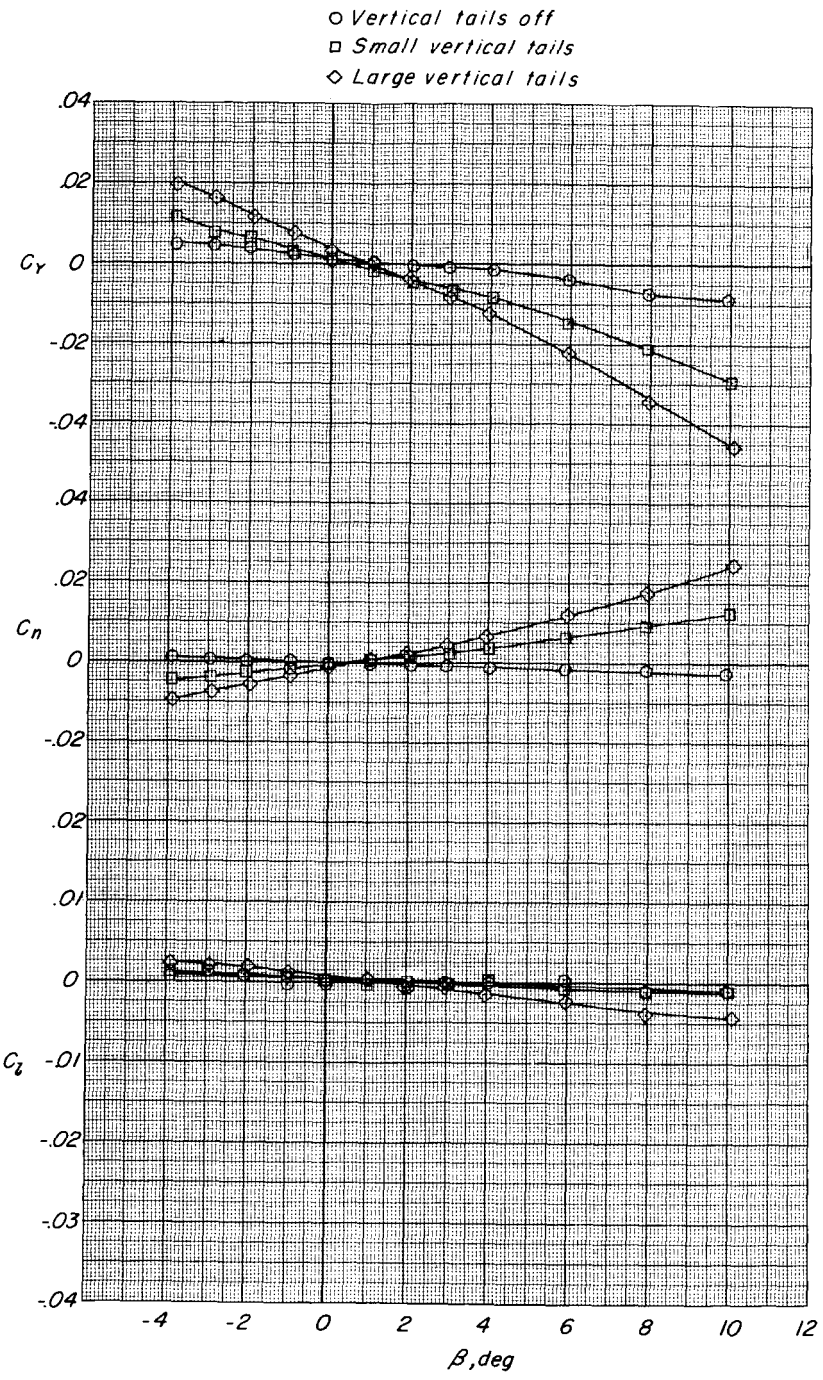

(a) $\alpha \approx 0^{\circ}$.

Figure 6.- Variation of static lateral stability characteristics with angle of sideslip.

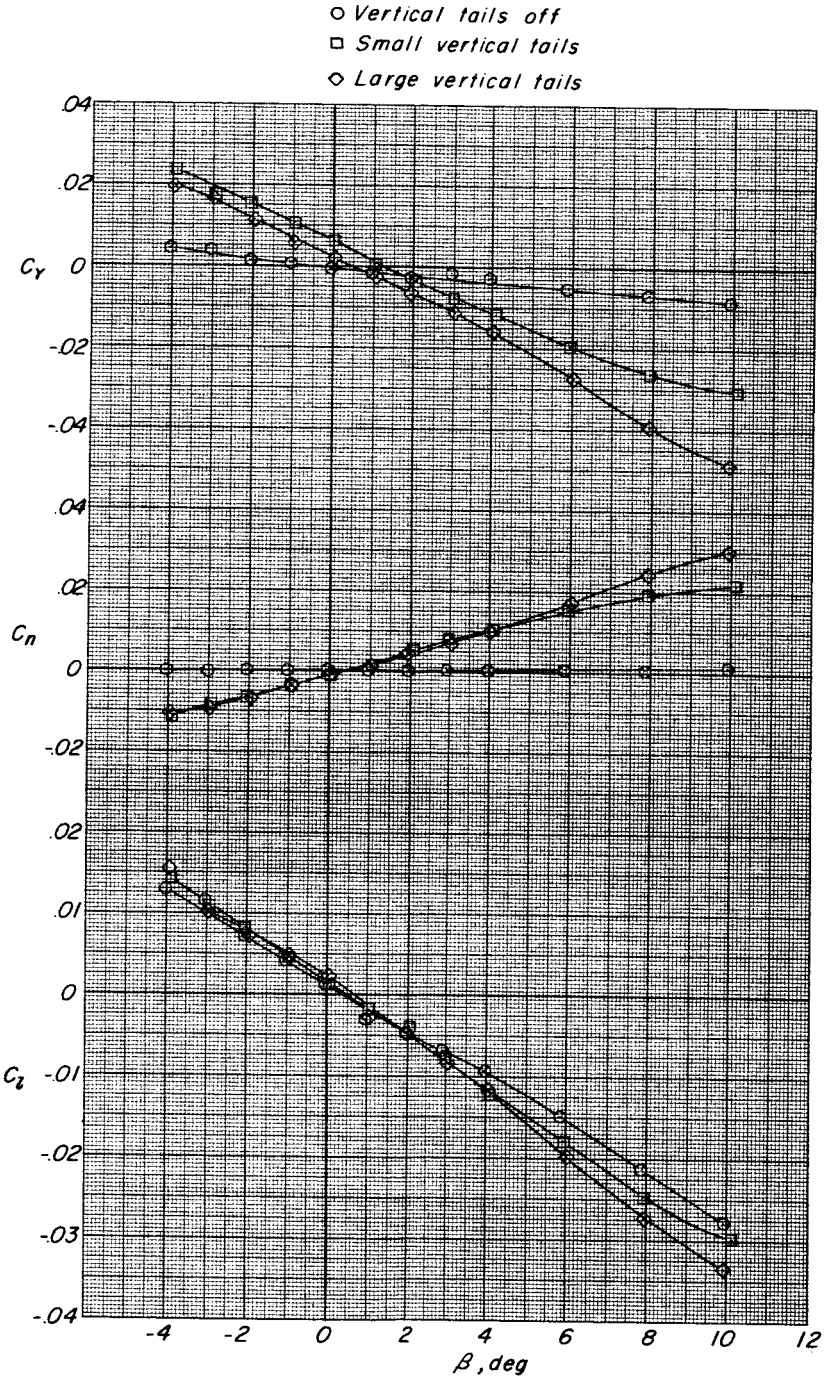

(b) $\alpha = 9^\circ$.

Figure 6.- Continued.

[redacted]

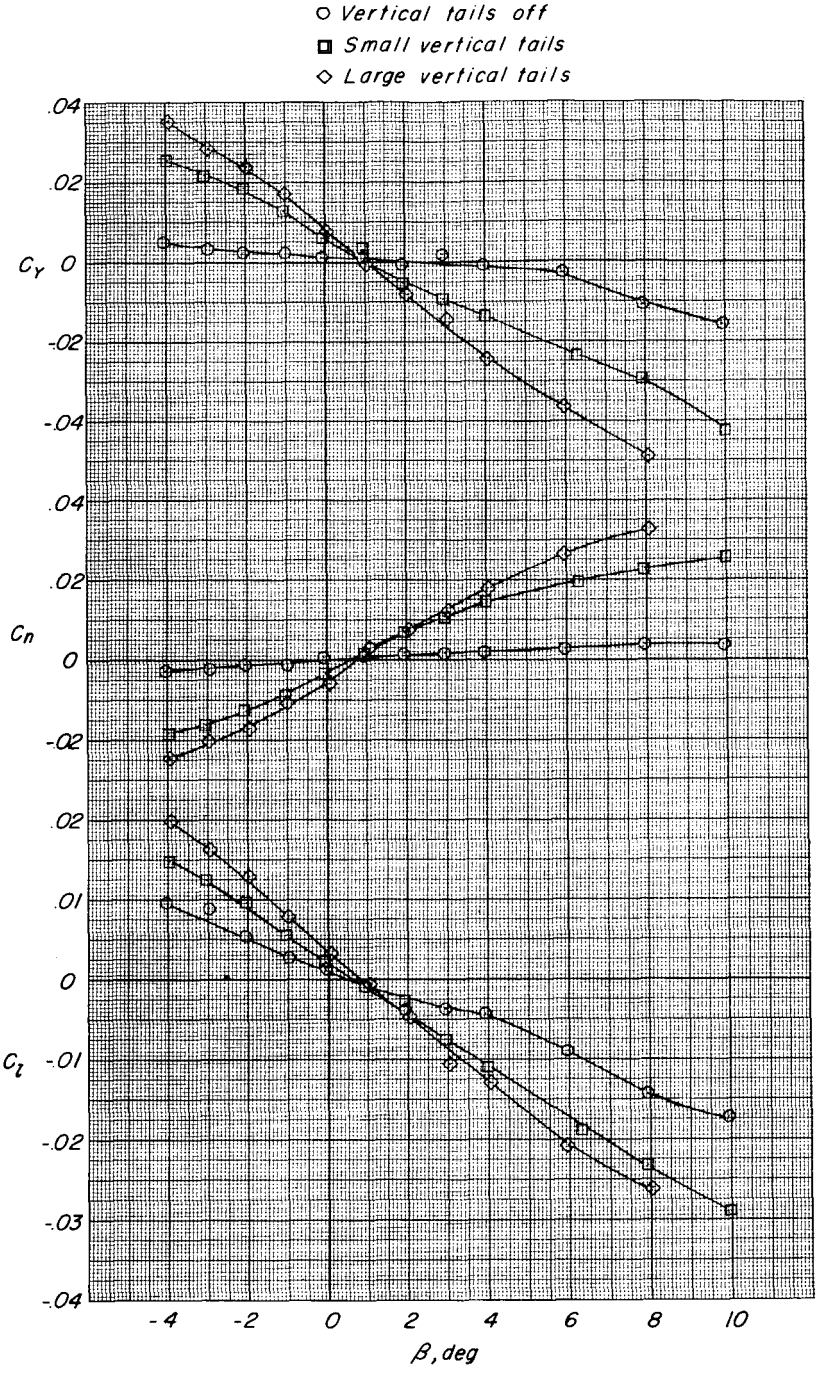

(c) $\alpha = 18^{\circ}$.

Figure 6.- Concluded.

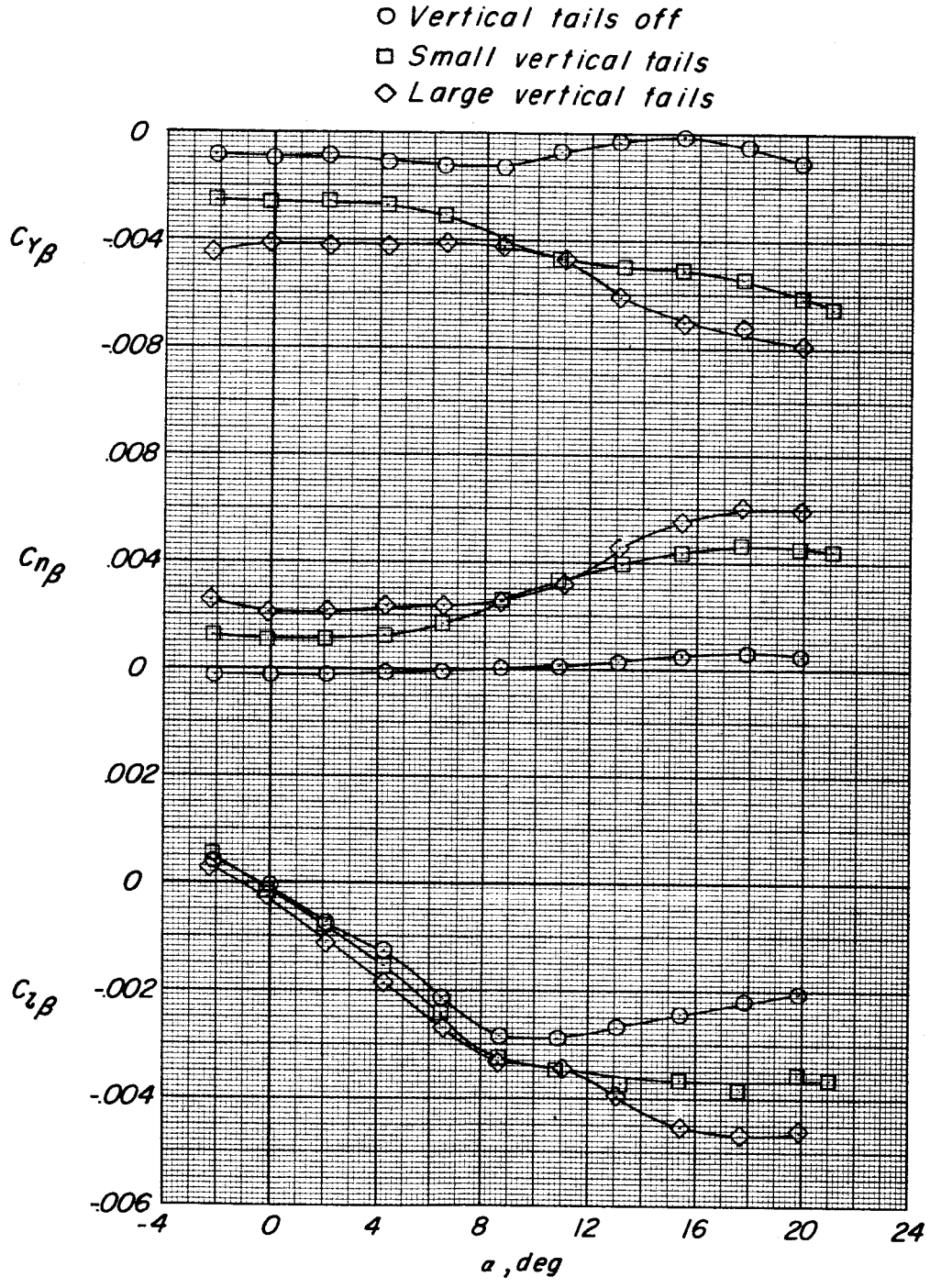

Figure 7.- Variation of static lateral stability derivatives with angle of attack. $\beta = \pm 4^\circ$.

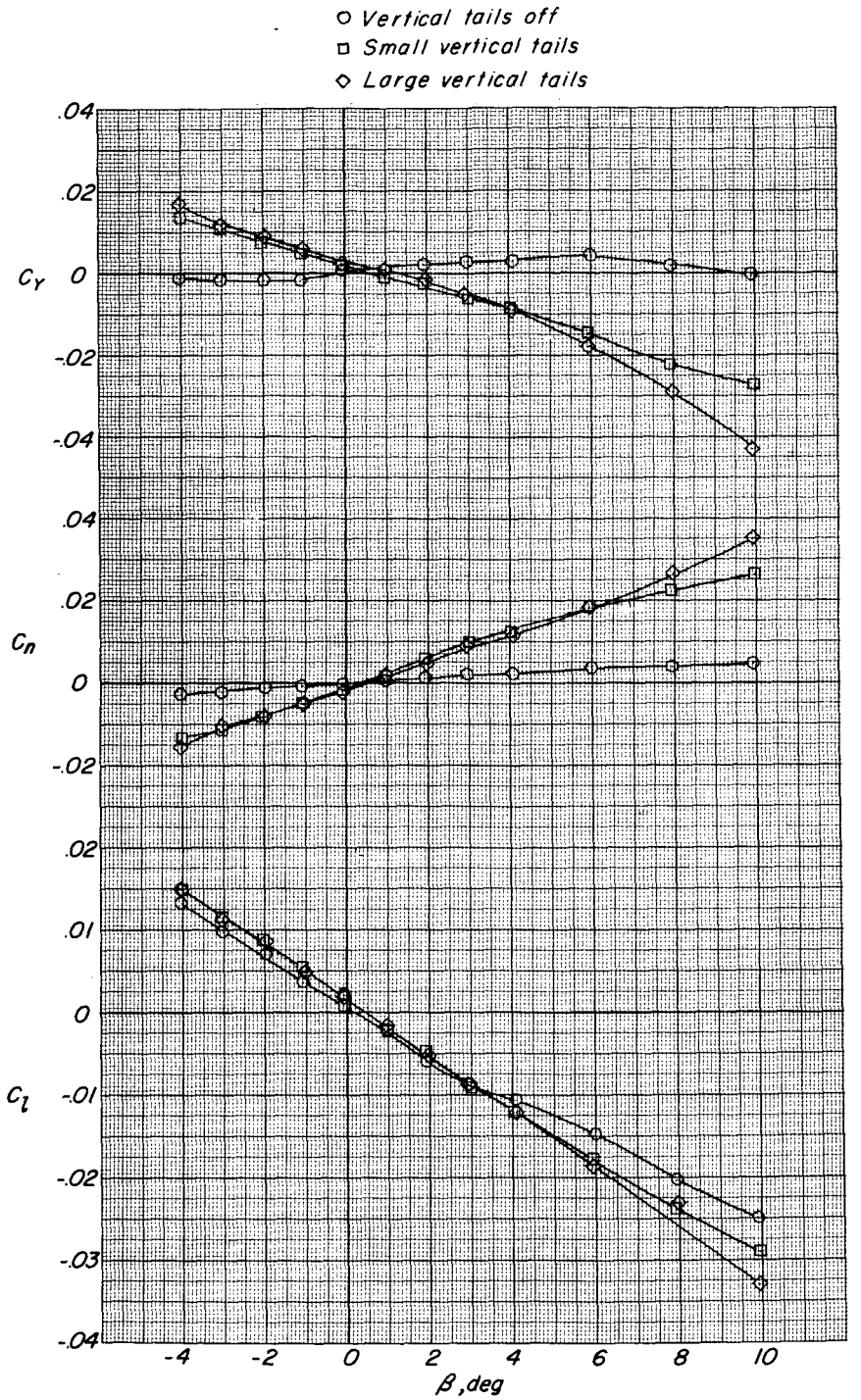

Figure 8.- Variation of static lateral stability characteristics with angle of sideslip with canard surface off. $\alpha = 9^{\circ}$.